Sensors and Materials, Vol. 38, No. 2 (2026) 539–544
MYU Tokyo

S & M 4318

Dosimetric Properties of Tm-doped $CaGdAlO_4$

Yuma Takebuchi,[1*] Daisuke Nakauchi,[2] Takumi Kato,[2]
Noriaki Kawaguchi,[2] and Takayuki Yanagida[2]

[1]Faculty of Engineering, Utsunomiya University, 7-1-2 Yoto, Utsunomiya, Tochigi 321-8585, Japan
[2]Nara Institute of Science and Technology (NAIST), Ikoma, Nara 630-0192, Japan

(Received October 31, 2025; accepted December 22, 2025)

Keywords: $CaGdAlO_4$, floating zone method, dosimetry, TSL

The photoluminescence (PL) and dosimetric properties of Tm-doped $CaGdAlO_4$ single crystals were investigated. The samples exhibited the luminescence arising from the 4f–4f transitions of Tm^{3+}. Thermally stimulated luminescence (TSL) glow curve measurements revealed that Tm doping into the $CaGdAlO_4$ lattice introduced new trapping centers. The 1% Tm-doped $CaGdAlO_4$ showed the highest TSL intensity as well as PL quantum yield. The minimum detectable dose in the TSL dose–response function of the 1% Tm-doped $CaGdAlO_4$ was 1 mGy.

1. Introduction

Owing to the recent increase in the use of ionizing radiation, improving materials for radiation detection is a key issue. Dosimetric materials using optically or thermally stimulated luminescence (OSL or TSL) phenomena are applied to personal and environmental dose monitoring and imaging plates.[1–4] During OSL and TSL processes, the energy of ionizing radiation is converted to carriers and temporarily accumulated within the materials. The carriers are released upon optical or thermal stimulation at any time, emitting OSL or TSL signals. From the OSL and TSL signals, the total amount and spatial distribution of irradiated dose can be estimated. Today, C-doped Al_2O_3 and BeO are the most commonly used materials in dose monitoring but they have limited sensitivity.[5,6] In addition, Eu-doped BaFBr and Eu-doped CsBr, which are well-known materials for radiation imaging, are hygroscopic.[7,8] For the above reasons, researchers have been developing novel dosimetric materials.[9–18]

$CaGdAlO_4$ belongs to the rare-earth calcium aluminate family ($ABCO_4$) and is attracting attention for optical applications such as a laser medium.[19,20] In addition, its good luminescence properties, low environmental toxicity, high thermal and chemical stability, and high atomic number (Z_{eff} = 52.5) are suitable for dosimetric materials for imaging plates. Our previous study revealed that the Tb^{3+}-doped $CaGdAlO_4$ single crystal has high sensitivity for X-rays.[21] On the other hand, the rare-earth calcium aluminates tend to contain extra oxygens in the host lattice.[22] The extra oxygen oxidizes Tb^{3+} to nonluminescent Tb^{4+} and decreases the luminescence

*Corresponding author: e-mail: takebuchi@a.utsunomiya-u.ac.jp
https://doi.org/10.18494/SAM6081

ISSN 0914-4935
https://myukk.org/

efficiency.[23,24] Therefore, other activators that maintain the luminous valence state may possibly improve the efficiency. Tm in oxides is generally stable in the luminous Tm^{3+} state and is expected to emit photons effectively. In this study, Tm-doped $CaGdAlO_4$ single crystals were grown by the floating zone (FZ) method, and the dependences of their photoluminescence (PL) properties as well as dosimetric properties on the Tm concentration were investigated.

2. Materials and Methods

Tm-doped $CaGdAlO_4$ single crystals were synthesized by the FZ method. CaO, Gd_2O_3, Al_2O_3, and Tm_2O_3 powders (4N) were used as raw materials. The powders were weighed stoichiometrically in accordance with the chemical formula of $CaGd_{1-x}Tm_xAlO_4$. The nominal Tm concentrations were 0.5, 1, and 1.5%. Synthesized crystals were covered by graphite powder and annealed at 800 °C under reduced pressure to remove extra oxygen. Details of the sample preparation were described in our previous paper.[21] A part of each crystal was crushed into powder for X-ray diffraction measurement, which was performed using a diffractometer (Rigaku, MiniFlex600). Total transmittance spectra were measured using a spectrophotometer (Shimadzu, SolidSpec-3700). PL excitation and emission maps, as well as internal PL quantum yields (*QY*s), were measured using a Quantaurus-QY spectrometer (Hamamatsu Photonics, C11347). TSL glow curves were measured using a TSL reader (NanoGray, TL-2000).[25] The heating rate was 1 °C/s. TSL emission spectra were measured using our original setup.[26] TSL dose–response functions were determined using the integrated intensity of the TSL glow curves. Before TSL measurement, the samples were irradiated with X-rays using an X-ray generator (Spellman, XRB80P & N200X4550). The bias voltage was set to 40 kV. The irradiation dose was controlled by controlling the tube current and irradiation time, as shown in Table 1. Only for the 0.1 mGy irradiation, the distance between the X-ray generator and the samples was also adjusted.

3. Results and Discussion

Figure 1 shows the powder XRD patterns of the Tm-doped $CaGdAlO_4$ along with a reference pattern from the Crystallography Open Database (COD 24-0221). The diffraction patterns are consistent with the reference pattern. No impurity peaks are shown in Fig. 1, indicating that the synthesized crystals are single-phase $CaGdAlO_4$. Tm^{3+} (1.052 Å) is expected to substitute into the Gd^{3+} (1.107 Å) site because of their similar ionic radii and valence, although the peak positions remain constant regardless of Tm concentration.[27]

Figure 2 shows the total transmittance spectra of the Tm-doped $CaGdAlO_4$. All the samples show absorption peaks at 270 and 310 nm owing to the $^8S_{7/2}$ to $^6P_{7/2}$, ^6I_j transitions of host Gd^{3+}.[28,29] The 1 and 1.5% Tm-doped samples exhibit additional absorption peaks at 360, 470,

Table 1
Tube current and irradiation time of the X-ray generator for each irradiation dose.

Conditions	Dose (mGy)					
	0.1	1	10	100	1000	10000
Tube current (mA)	0.052	0.052	0.052	0.52	5.2	5.2
Irradiation time (s)	6	6	60	60	60	600

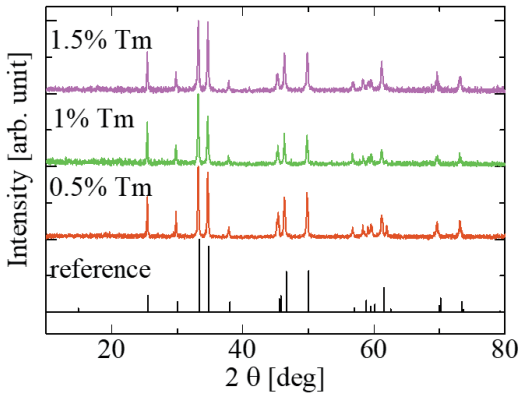

Fig. 1. (Color online) XRD patterns of Tm-doped $CaGdAlO_4$ with a reference pattern.

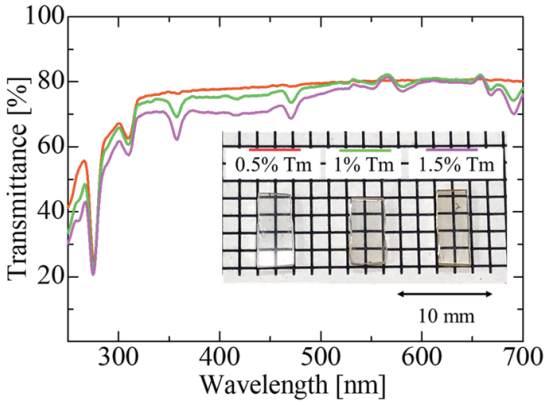

Fig. 2. (Color online) Total transmittance spectra of Tm-doped $CaGdAlO_4$.

and 690 nm attributed to the $^3H_6$–$^1D_2$, $^1G_4$, and $^3F_{2,3}$ transitions of Tm^{3+}, respectively.[28] The depth of the additional peaks increases as the Tm concentration increases. The overall transmittance of the samples is around 80% in the visible region. High transparency can be observed visibly, as shown in the inset of Fig. 2. On the other hand, the high-Tm-concentration samples show a broad absorption band at around 400 nm and slightly brown color. This absorption band would be due to extra oxygen at the interstitial site. According to a previous report,[30] when Gd^{3+} is substituted with Tm^{3+}, which is isovalent, or smaller ions, the void space of the interstitial site increases. Therefore, Tm^{3+} doping increases the amount of extra oxygen, and the conditions of reduction annealing for the high-Tm-concentration sample are insufficient.

Figure 3 shows the PL excitation and emission map of the 1% Tm-doped $CaGdAlO_4$. Here, the vertical and horizontal axes indicate the excitation and emission wavelengths, respectively, and the normalized intensities are indicated by a color scale. Upon excitation at 360 nm, luminescence peaks at around 470 and 800 nm are observed. The origins are attributed to the complex of the $^1D_2$–$^3F_4$ and $^1G_4$–$^3H_6$ transitions of Tm^{3+} and the $^3G_4$–$^3H_6$ transitions of Tm^{3+}.[31–33] In addition, an emission peak at around 740 nm is also observed, the origin of which would be the ^2E–$^4A_2$ transitions of Cr^{3+} unexpected impurities.[34] All Tm-doped $CaGdAlO_4$ samples show the same emission bands. The PL *QY*s of the 0.5, 1, and 1.5% Tm-doped $CaGdAlO_4$ are 9.1, 23.2, and 13.8%, respectively.

Figure 4 shows the TSL glow curves of the Tm-doped $CaGdAlO_4$ after X-ray irradiation at 10 Gy. In our previous reports, undoped $CaGdAlO_4$ and $CaYAlO_4$ exhibited a glow peak at 80–90 °C.[21,23] The 0.5% Tm-doped $CaGdAlO_4$ shows a glow peak at the same temperature region. The origin is considered to be an intrinsic $ABCO_4$ host defect. The glow peak shifts slightly toward higher temperatures with Tm doping. In addition, a glow peak at around 200 °C appears in the 1 and 1.5% Tm-doped $CaGdAlO_4$. The result indicates that Tm doping generates new trapping centers at slightly higher than 100 °C and around 200 °C. A candidate for the origin of the glow peaks is cation vacancies. The segregation coefficient of Tm^{3+} in $CaGdAlO_4$ actually has been determined as 0.61.[35] Thereby, cation vacancies are generated during crystal growth, and new trapping centers may be introduced. The high temperature peaks are advantages for fading properties. The trend of the TSL intensities is consistent with that of the PL *QY*s, and the 1% Tm-doped $CaGdAlO_4$ shows the highest TSL intensity.

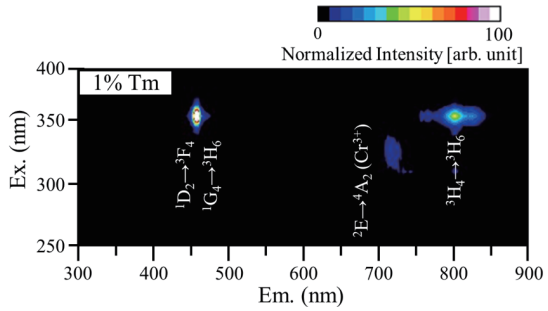

Fig. 3. (Color online) PL excitation and emission map of 1% Tm-doped $CaGdAlO_4$. The vertical and horizontal axes indicate excitation and emission wavelengths, respectively.

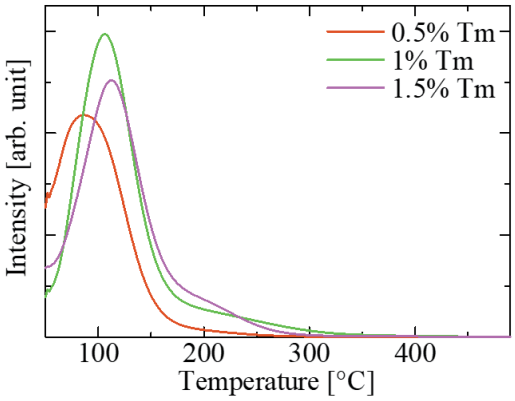

Fig. 4. (Color online) TSL glow curves of Tm-doped $CaGdAlO_4$.

Figure 5 shows the TSL emission spectra of the Tm-doped $CaGdAlO_4$. The inset shows the enlarged view between 300 and 520 nm. Upon heat stimulation of 100 °C, the samples show five emission peaks at 370, 460, 475, 740, and 800 nm. The results of PL indicate the origins to be the $^1D_2$–$^3F_6$, $^1D_2$–$^3F_4$, $^1G_4$–$^3H_6$, and $^3H_4$–$^3H_6$ transitions of Tm^{3+} for the peaks at 370, 460, 475, and 800 nm, respectively, and the ^2E–$^4A_2$ transitions of Cr^{3+} for the 740 nm peak. Compared with PL spectra, the relative intensity ratio between the PL and TSL spectra is different because of the different excitation processes. In the PL process, activator ions are directly excited by excitation photons. In the TSL process, however, activator ions are excited by carriers released from trapping centers. Therefore, the excitation energies in each process are different. In fact, the $^3H_4$–$^3H_6$ transitions of Tm^{3+} and the ^2E–$^4A_2$ transitions of Cr^{3+} also occur by other excitation energies although the PL emission maps have been measured under only 250–400 nm excitation in this study.[32,34] For the above reason, emissions at around 740 and 800 nm are dominant in the TSL process.

Figure 6 shows the TSL dose–response function of the 1% Tm-doped $CaGdAlO_4$, which shows the highest TSL intensity. The minimum detectable dose (MDD) is 1 mGy in the 1% Tm-doped $CaGdAlO_4$. This value is worse than those of our previous Tb-doped $CaGdAlO_4$ and practical TSL materials, whereas the PL *QY*s of the Tb- and Tm-doped samples are almost the same.[21,36] Actually, the TSL reader for the TSL glow curves and dose–response function cuts luminescence exceeding 520 nm to avoid black body radiation. From the TSL emission spectra, however, most carriers are converted to 740 and 800 nm photons, and the luminescence below 520 nm is weak. Thereby, the TSL efficiency is underestimated in this measurement. Choosing a suitable dopant without red luminescence and preventing Cr^{3+} impurities by using high-purity raw materials may possibly improve the TSL signal of $CaGdAlO_4$.

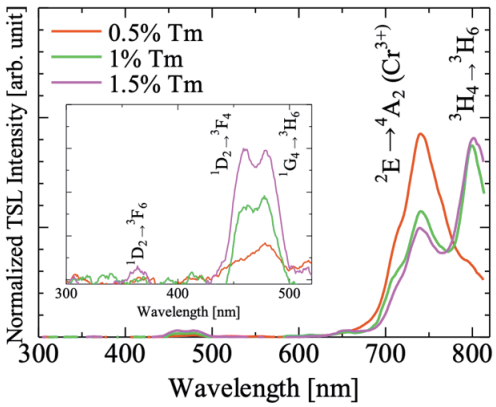

Fig. 5. (Color online) TSL emission spectra of Tm-doped $CaGdAlO_4$. Inset shows the enlarged view between 300 and 520 nm.

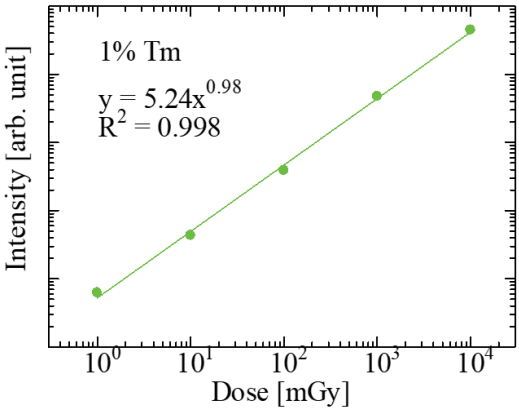

Fig. 6. (Color online) TSL dose–response function of 1% Tm-doped $CaGdAlO_4$.

4. Conclusions

In this study, the PL and TSL properties of Tm-doped $CaGdAlO_4$ single crystals were examined. By the FZ method, we successfully synthesized transparent and single-phase $CaGdAlO_4$. The Tm-doped $CaGdAlO_4$ exhibited luminescence originating from the 4f–4f transitions of Tm^{3+}, and Tm doping up to 1% increased the PL *QY*. In TSL glow curve measurements, the 1 and 1.5% Tm-doped $CaGdAlO_4$ showed a glow peak at around 200 °C in addition to the glow peak at around 90 °C owing to intrinsic host defects. One of the candidates for the new trapping center is cation vacancies introduced by Tm doping. The 1% Tm-doped $CaGdAlO_4$ exhibited the highest TSL intensity owing to the highest PL *QY* and the increased trapping probability. The MDD of the 1% Tm-doped $CaGdAlO_4$ was determined to be 1 mGy.

Acknowledgments

This work was supported by the Iwatani Naoji Foundation, the Cooperative Research Project of the Research Center for Biomedical Engineering, the Murata Foundation, the Tochigi Industrial Promotion Center, and the Utsunomiya University Research Grant.

References

1 H. Nanto: Sens. Mater. **30** (2018) 327. https://doi.org/10.18494/SAM.2018.1803
2 H. Nanto and G. Okada: Jpn. J. Appl. Phys. **62** (2023) 010505. https://doi.org/10.35848/1347-4065/ac9106
3 K. Shinsho, R. Oh, M. Tanaka, N. Sugioka, H. Tanaka, G. Wakabayashi, T. Takata, W. Chang, S. Matsumoto, G. Okada, S. Sugawara, E. Sasaki, K. Watanabe, Y. Koba, K. Nagasaka, S. Yoshihashi, A. Uritani, and T. Negishi: Jpn. J. Appl. Phys. **62** (2023) 010502. https://doi.org/10.35848/1347-4065/ac971e
4 E. G. Yukihara, S. W. S. McKeever, C. E. Andersen, A. J. J. Bos, I. K. Bailiff, E. M. Yoshimura, G. O. Sawakuchi,L. Bossin, and J. B. Christensen: Nat. Rev. Methods Prim. **2** (2022) 26. https://doi.org/10.1038/s43586-022-00102-0
5 A. K. Singh, N. S. Rawat, B. Dhabekar, J. P. Nair, S. Dawn, D. R. Mishra, and B. K. Sapra: Radiat. Phys. Chem. **211** (2023) 111041. https://doi.org/10.1016/j.radphyschem.2023.111041
6 E. Bulur and B. E. Saraç: Radiat. Meas. **59** (2013) 129. https://doi.org/10.1016/j.radmeas.2013.04.009

7 G. Fiksel, F. J. Marshall, C. Mileham, and C. Stoeckl: Rev. Sci. Instrum. **83** (2012) 086103. https://doi.org/10.1063/1.4739771
8 N. Kurata, N. Kubota, Y. Takei, and H. Nanto: Radiat. Prot. Dosimetry **119** (2006) 398. https://doi.org/10.1093/rpd/nci515
9 Y. Takebuchi, M. Morioka, Y. Nakashima, K. Tezuka, H. Kimura, S. Otake, and T. Yanagida: Sens. Mater. **37** (2025) 525. https://doi.org/10.18494/SAM5437
10 T. Kato, A. Nishikawa, D. Nakauchi, N. Kawaguchi, and T. Yanagida: Sens. Mater. **37** (2025) 475. https://doi.org/10.18494/SAM5424
11 A. Nishikawa, K. Ichiba, T. Kato, D. Nakauchi, N. Kawaguchi, and T. Yanagida: Sens. Mater. **37** (2025) 569. https://doi.org/10.18494/SAM5429
12 H. Ezawa, T. Kato, Y. Takebuchi, K. Okazaki, K. Ichiba, D. Nakauchi, N. Kawaguchi, and T. Yanagida: Sens. Mater. **37** (2025) 581. https://doi.org/10.18494/SAM5431
13 H. Kimura, T. Fujiwara, H. Kato, M. Koshimizu, G. Wakabayashi, Y. Takebuchi, T. Kato, D. Nakauchi, N. Kawaguchi, and T. Yanagida: Sens. Mater. **37** (2025) 599. https://doi.org/10.18494/SAM5442
14 H. Ezawa, Y. Takebuchi, K. Okazaki, T. Kato, D. Nakauchi, N. Kawaguchi, and T. Yanagida: Sens. Mater. **36** (2024) 465. https://doi.org/10.18494/SAM4757
15 S. Otake, H. Sakaguchi, Y. Yoshikawa, T. Kato, D. Nakauchi, N. Kawaguchi, and T. Yanagida: Sens. Mater. **36** (2024) 539. https://doi.org/10.18494/SAM4759.
16 M. Koshimizu, K. Oba, Y. Fujimoto, and K. Asai: Sens. Mater. **36** (2024) 565. https://doi.org/10.18494/SAM4761.
17 Y. Takebuchi, M. Koshimizu, T. Kato, D. Nakauchi, N. Kawaguchi, and T. Yanagida: J. Lumin. **251** (2022) 119247. https://doi.org/10.1016/j.jlumin.2022.119247
18 Y. Takebuchi, T. Kato, D. Nakauchi, N. Kawaguchi, and T. Yanagida: Sens. Mater. **34** (2022) 645. https://doi.org/10.18494/SAM3685
19 P. Loiko, F. Druon, P. Georges, B. Viana, and K. Yumashev: Opt. Mater. Express **4** (2014) 2241. https://doi.org/10.1364/OME.4.002241
20 S. Li, Y. Yang, S. Zhang, T. Yan, N. Ye, and Y. Hang: J. Lumin. **228** (2020) 117620. https://doi.org/10.1016/j.jlumin.2020.117620
21 Z. Aoki, Y. Takebuchi, D. Nakauchi, T. Kato, N. Kawaguchi, and T. Yanagida: Nucl. Instruments Methods Phys. Res. Sect. B Beam Interact. with Mater. Atoms **547** (2024) 165182. https://doi.org/10.1016/j.nimb.2023.165182
22 Q. Hu, Z. Jia, C. Tang, N. Lin, J. Zhang, N. Jia, S. Wang, X. Zhao, and X. Tao: CrystEngComm **19** (2017) 537. https://doi.org/10.1039/C6CE02411D
23 Z. Aoki, Y. Takebuchi, D. Nakauchi, T. Kato, N. Kawaguchi, and T. Yanagida: Opt. Mater. (Amst). **134** (2022) 113068. https://doi.org/10.1016/j.optmat.2022.113068
24 Z. Aoki, Y. Takebuchi, D. Nakauchi, T. Kato, N. Kawaguchi, and T. Yanagida: J. Mater. Sci. Mater. Electron. **34** (2023) 2021. https://doi.org/10.1007/s10854-023-11442-2
25 T. Yanagida, Y. Fujimoto, N. Kawaguchi, and S. Yanagida: J. Ceram. Soc. Japan **121** (2013) 988. https://doi.org/10.2109/jcersj2.121.988
26 G. Okada, T. Kato, D. Nakauchi, K. Fukuda, and T. Yanagida: Sens. Mater. **28** (2016) 897. https://doi.org/10.18494/SAM.2016.1250
27 R. D. Shannon: Acta Crystallogr. Sect. A **32** (1976) 751. https://doi.org/10.1107/S0567739476001551
28 Z. Pan, P. Loiko, S. Slimi, H. Yuan, Y. Wang, Y. Zhao, P. Camy, E. Dunina, A. Kornienko, L. Fomicheva, L. Wang, W. Chen, U. Griebner, V. Petrov, R. M. Solé, F. Díaz, M. Aguiló, and X. Mateos: J. Lumin. **246** (2022) 118828. https://doi.org/10.1016/j.jlumin.2022.118828
29 E. Haruaki, Y. Takebuchi, K. Okazaki, K. Ichiba, T. Kato, D. Nakauchi, N. Kawaguchi, and T. Yanagida: Radiat. Phys. Chem. **220** (2024) 111721. https://doi.org/10.1016/j.radphyschem.2024.111721
30 G. Nirala, D. Yadav, and S. Upadhyay: J. Adv. Ceram. **9** (2020) 129. https://doi.org/10.1007/s40145-020-0365-x.
31 Y. Takebuchi, H. Fukushima, T. Kato, D. Nakauchi, N. Kawaguchi, and T. Yanagida: Sens. Mater. **32** (2020) 1405. https://doi.org/10.18494/SAM.2020.2717
32 T. Yanagida, K. Okazaki, D. Nakauchi, T. Kato, and N. Kawaguchi: Jpn. J. Appl. Phys. **64** (2025) 07SP15. https://doi.org/10.35848/1347-4065/aded99
33 D. Nakauchi, T. Kato, N. Kawaguchi, and T. Yanagida: Sens. Mater. **37** (2025) 547. https://doi.org/10.18494/SAM5425
34 Z. Zhang, Y. Huang, L. Zhang, S. Sun, F. Yuan, and Z. Lin: J. Cryst. Growth **463** (2017) 33. https://doi.org/10.1016/j.jcrysgro.2017.01.055
35 J. Di, X. Xu, C. Xia, Q. Sai, D. Zhou, Z. Lv, and J. Xu: J. Lumin. **155** (2014) 101. https://doi.org/10.1016/j.jlumin.2014.06.010
36 A. Fujii, K. Miyazaki, Y. Takebuchi, T. Kato, D. Nakauchi, N. Kawaguchi, and T. Yanagida: Opt. Mater. (Amst). **169** (2026) 117677. https://doi.org/10.1016/j.optmat.2025.117677